

Investigating tissue respiration and skin microhaemocirculation under adaptive changes and the synchronization of blood flow and oxygen saturation rhythms

A V Dunaev^{1,2}, V V Sidorov³, A I Krupatkin⁴, I E Rafailov⁵,
S G Palmer^{1,5}, N A Stewart^{1,5}, S G Sokolovski¹
and E U Rafailov¹

¹ Photonics and Nanoscience Group, Division of Physics, School of Engineering, Physics and Mathematics, University of Dundee, Dundee DD1 4HN, UK

² State University—Education-Science-Production Complex, Scientific-Educational Center of ‘Biomedical Engineering’, Oryol 302020, Russia

³ SPE ‘LAZMA’ Ltd, Moscow 125252, Russia

⁴ Priorov Central Research Institute of Traumatology and Orthopaedics, Moscow 127299, Russia

⁵ Division of Imaging and Technology, School of Medicine, University of Dundee, Dundee DD1 9SY, UK

E-mail: a.v.dunaev@dundee.ac.uk

Received 23 October 2013, revised 6 February 2014

Accepted for publication 11 February 2014

Published 12 March 2014

Abstract

Multi-functional laser non-invasive diagnostic systems allow the study of a number of microcirculatory parameters, including index of blood microcirculation (I_m) (by laser Doppler flowmetry, LDF) and oxygen saturation (S_tO_2) of skin tissue (by tissue reflectance oximetry, TRO). This research aimed to use such a system to investigate the synchronization of microvascular blood flow and oxygen saturation rhythms under normal and adaptive change conditions. Studies were conducted on eight healthy volunteers of 21–49 years. These volunteers were observed between one and six months, totalling 422 basic tests (3 min each). Measurements were performed on the palmar surface of the right middle finger and the lower forearm’s medial surface. Rhythmic oscillations of LDF and TRO were studied using wavelet analysis. Combined tissue oxygen consumption data for all volunteers during ‘adaptive changes’ increased relative to normal conditions with and without arteriovenous anastomoses. Data analysis revealed resonance and synchronized rhythms in microvascular blood flow and oxygen saturation as an adaptive change in myogenic oscillation (vasomotion) resulting from exercise and possibly

psychoemotional stress. Synchronization of myogenic rhythms during adaptive changes may lead to increased oxygen consumption as a result of increased microvascular blood flow velocity.

Keywords: laser Doppler flowmetry, tissue reflectance oximetry, vasomotion, oxygen consumption, adaptive changes

1. Introduction

The evaluation of stress-induced adaptive changes in the tissue respiration and circulatory systems of individuals may provide important information for studies in physiology and clinical medicine. Optical techniques are one of the most promising non-invasive technologies for the diagnosis of medical conditions. The fields of photonics and biophotonics have witnessed real progress and accomplishments. This has led to the development and introduction of novel and compact non-invasive optical diagnostic devices into biomedicine. Especially, progress has been achieved in developing methods and devices for non-invasive studies of blood flow (Zakharov *et al* 2009, 2011) as well as quantitative assessment and imaging associated with this (Kalchenko *et al* 2011, 2012, Fine *et al* 2012, Daly *et al* 2013). However, these methods and devices do not allow full analysis of the consumption and utilization of oxygen in tissue, as well as frequency modulation rhythms of blood flow and tissue oxygen saturation. Simultaneous use of several methods, such as the laser Doppler flowmetry (LDF) for the measurement of tissue perfusion and absorption spectroscopy for the analysis of tissue oxygenation, can provide additional information about the different types and features of oscillation hemodynamics in the same diagnostic tissue volume (Thorn *et al* 2009). The recent development of multi-functional non-invasive laser based diagnostic systems, such as the 'LAKK-M' (SPE 'LAZMA' Ltd, Russia) (Rogatkin *et al* 2010, 2011), has made it possible to conduct simultaneous real-time studies on a number of tissue parameters, including microvascular blood flow (by LDF) and oxygen saturation of skin tissue (by tissue reflectance oximetry, TRO) (Rogatkin and Lapaeva 2003, Stewart *et al* 2012, Dunaev *et al* 2013). This diagnostic system can be applied in angiology and physiology for studying the status of the microvascular tone and analyzing the neurophysiological mechanisms of regulatory microhemodynamics, in oncology and radiology for identification of the oxygen status of the tumour and the prognosis of radiation treatment, and in transplantation for assessment of graft acceptance and tissue viability.

The results of LDF measurements, representing 'index of blood microcirculation (I_m)' or 'perfusion', assessed in conventional (arbitrary) perfusion units (PU), reveal a complex, non-periodic process. This variable component contains information on the modulation of blood flow. Use of spectral signal processing algorithms on LDF-graphs for decoding and analysis provides information about the condition of vascular tone in terms of its contribution to the different mechanisms of microhemodynamic regulation (Bracic and Stefanovska 1998, Krupatkin and Sidorov 2005). Oscillatory processes play an important role in the functioning of the system of tissue microcirculation (Stefanovska *et al* 1999, Bernjak *et al* 2005, Krupatkin 2007, 2011). Several frequency ranges of blood flow oscillations in microvascular networks, each of a different regulatory origin, have been identified (endothelial, neurogenic, myogenic, etc) (Kvernmo *et al* 1999, Kvandal *et al* 2006, Krupatkin 2011). Many medical publications are devoted to the study of myogenic oscillations, because they characterize the state of pre-capillary sphincters, which play an important role in the regulation of blood flow

(Schmidt-Lucke *et al* 2002, Graaff *et al* 2007, Schmiedel *et al* 2007, Rossi *et al* 2008, 2013, Newman *et al* 2009).

TRO is based on the principles of absorption spectroscopy and allows non-invasive (*in vivo*, transcutaneous) monitoring of microhemodynamics and oxygen transport and utilization within the entire blood microcirculation system. Using and comparing this technique with the method of pulse oximetry, which only measures oxygen saturation in arterial blood (S_aO_2), provides much more information for clinical medicine (Amzina *et al* 2006, Colquhoun *et al* 2012, Quaresima *et al* 2013). TRO determines the relative volume of all fractions of haemoglobin (total haemoglobin) in a tissue volume (average level of blood volume: V_b , in percent) and oxygen saturation of the microvasculature, generally containing arterioles with oxyhaemoglobin and venules with deoxyhaemoglobin (average level of tissue oxygen saturation: S_tO_2 , in percent). It should be noted that the changes in tissue oxygen saturation are essentially the increases and decreases of tissue oxygen consumption. There are few studies of rhythms (for example, spectral processing algorithms) within these recorded TRO-signals (Coca *et al* 1998, 2000, Stefanovska 2009, Thorn *et al* 2009), and literature reporting the relationships between I_m and S_tO_2 -graphs are rare (Tyrrell *et al* 2011, Bernjak *et al* 2012). In isolated cases it has been used to assess vasomotion and myogenic rhythms for perfusion and tissue oxygen saturation, for example (Thorn *et al* 2011). Here we propose that, similarly to the LDF plots, the analysis of oscillation signals recorded by TRO is of practical interest in studying the parameters of microcirculation of blood. This is particularly important as the relationships between LDF and TRO attract increasing attention from researchers in the field.

The aim of this research was to use LDF- and TRO-graphs to investigate tissue respiration during the synchronization of microvascular blood flow and oxygen saturation rhythms under normal conditions and during adaptive changes.

2. Methods and materials

In this study we used a 'LAKK-M' system, which, besides LDF and TRO, contains pulse oximetry and laser fluorescence diagnostic channels (Dunaev *et al* 2013) (figure 1). This system includes near-infrared (1064 nm), red (640 nm) and green (532 nm) lasers for LDF- and TRO-channels and allows simultaneous recording of the I_m , S_tO_2 and V_b parameters in a tissue volume about 3–5 mm³ (with the separation distance between the source and detector fibers at around 1 mm).

The LDF channel used traditional methodology, with the results of perfusion in accordance with the following well known equation (Obeid 1993, Leahy and Nilsson 2010):

$$I_m = \frac{k \int f \cdot V(f) df}{\int V(f) df}, \quad (1)$$

where k is the coefficient of the device (calibration factor), f is the value of the Doppler frequency and the $V(f)$ is the Doppler signal amplitude.

The TRO channel of the 'LAKK-M' system calculates the parameters S_tO_2 and V_b according to the following methodology. Tissue oxygen saturation is defined as the percentage composition of oxyhaemoglobin in the sum of only two haemoglobin fractions—oxyhaemoglobin and deoxyhaemoglobin (Krupatkin *et al* 2007):

$$S_tO_2 = \frac{C_{HbO_2}}{C_{HbO_2} + C_{Hb}} \cdot 100\%, \quad (2)$$

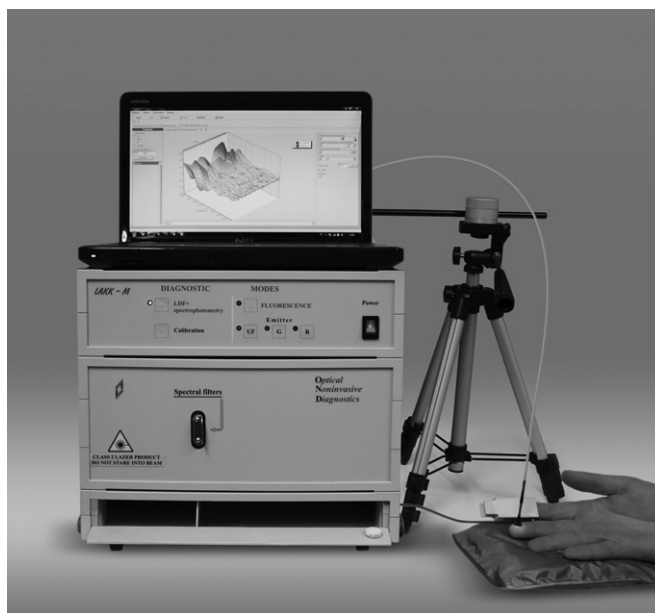


Figure 1. The multi-functional laser non-invasive diagnostic system ‘LAKK-M’.

where, if the molar concentration of HbO₂ in the blood is designated as C_{HbO₂} and the overall molar concentration of all the fractions of haemoglobin in the blood, including HbO₂, is designated as the sum of C_{HbO₂} and C_{Hb}, then the parameter V_b can be calculated as follows:

$$V_b = \frac{C_{Hb} + C_{HbO_2}}{C_{Hb} + C_{HbO_2} + C_{other}} \cdot 100\%, \quad (3)$$

where C_{other} is the molar concentration of all secondary cellular structures in the examined volume of tissue.

The value of the molar concentration is determined by the absorption by biological tissue of radiation at different wavelengths. On the basis of the well-known Beer–Lambert law and taking into account multicomponent biotissue, the absorption coefficient can be calculated using the following formula:

$$\mu_a(\lambda) = \sum_i \varepsilon_i(\lambda) \cdot C_i, \quad (4)$$

where $\varepsilon_i(\lambda)$ is the molar extinction coefficient for the biochemical medium component *i*, while C_{*i*} is the molar concentration of component *i* in the tested region.

During the implementation of the TRO function of this device, two wavelengths (640 and 532 nm) are used. Taking into account certain restrictions, the molar concentrations of haemoglobin fractions vital for the calculation of S_tO₂ and V_b can be calculated using the following equations (Khalil 2006, Heusmann *et al* 1996):

$$\begin{aligned} \mu_a(\lambda_1) &= \varepsilon_{Hb}(\lambda_1) \cdot C_{Hb} + \varepsilon_{HbO_2}(\lambda_1) \cdot C_{HbO_2} + \varepsilon_{other}(\lambda_1) \cdot C_{other}, \\ \mu_a(\lambda_2) &= \varepsilon_{Hb}(\lambda_2) \cdot C_{Hb} + \varepsilon_{HbO_2}(\lambda_2) \cdot C_{HbO_2} + \varepsilon_{other}(\lambda_2) \cdot C_{other}, \end{aligned} \quad (5)$$

where $\varepsilon_{other}(\lambda_j)$ is the sum molar extinction coefficient of light at different wavelengths by all other skin structures.

Studies of different durations were conducted with eight volunteers with no history of cardiovascular disease and without chronic diseases and medication, aged 21–49 years,

Table 1. Volunteer and study data.

No volunteer	Age, years	Sex	Duration of studies, months	Number of basic tests		Number of occlusion tests	Number of studies after sport
				With AVAs	Without AVAs		
1	36	Male	6	80	41	–	20
2	29	Female	1	19	–	20	–
3	49	Male	2	23	5	–	–
4	20	Male	1	18	14	–	–
5	23	Male	2	27	25	–	–
6	29	Female	4	34	31	–	–
7	24	Female	2	22	21	–	–
8	23	Male	3	25	17	–	–
Total:	29 ± 9.5	–	–	248	154	20	20 422

comprising three females and five males (table 1). These studies involved simultaneously recording the parameters of LDF (I_m), TRO (S_rO_2) and pulse oximetry (S_aO_2). In order to assess the I_m and the S_rO_2 oscillatory component, spectral wavelet analysis of oscillations was used (software 3.0.2.384, LAZMA, Russia). This program uses a continuous wavelet transform, with the Morle complex valued wavelet being used as the analysing wavelet (Tankanag and Chemeris 2008, Tankanag and Chemeris 2009). The study was performed approximately at the same time of day (around 12:00) to avoid circadian rhythms influence on the blood circulation, at ambient room temperature (21–22 °C) in a sitting position after a 30 min rest period (allowed for acclimatization). The temperature of the volunteers was measured on the tested regions of skin by an infrared clinical thermometer ‘Medisana’ 76120 (FTN). All temperatures recorded were within the range of 34–36 °C. The measurements were performed on the inner (palmar) surface of the right middle finger. This area was chosen because it is rich in arteriovenous anastomoses (AVAs) and variability of the LDF signal is less than in tissue with fewer shunts (Salerud *et al* 1983). It should be emphasized that this area is regulated almost exclusively by the autonomic nervous system and is very responsive to adaptive changes. In addition, studies were conducted in an area almost completely devoid of AVAs: the lower forearm’s medial surface (the skin without AVAs), characterized by greater nutritive blood flow. The necessary calibration of the ‘LAKK-M’ system was carried out prior to each study by using a specific fluoroplastic (PTFE) template located at the bottom of the device. This follows the calibration protocol detailed in the manual for the ‘LAKK-M’ system. The technical characteristics of the device were stable at all times. Immobility of the optical probe on the surface of the skin was ensured according to the user manual.

It should be noted that for a versatile study of adaptive changes of microcirculation under stressful conditions, a part of the volunteers were studied for a longer duration of time and at different physical activities. Moreover, even with a short period of research of some volunteers (1–2 months) taking measurements in two areas of the skin and using physiological tests, has provided a sufficient number of measurements (no less 28 for each volunteer) for the proposed research.

Thus, the male participant of 36 years (volunteer no 1) was studied over the course of six months, totalling 100 records in the skin with AVAs ($n = 100$): 60 basic tests for 3 min, plus 20 ‘before and after’ records to monitor the effects of exercise, in this case swimming (500 m) with the water temperature in the pool about 24–28 °C, which can be considered a form of stress for the study of the adaptive changes. Readings were taken after a rest period of

20–30 min after the exercise, with the temperatures being recorded prior to each one falling in the range of 34–35 °C. It should be noted that the use of LDF and TRO to investigate the blood microcirculation system was done over a duration of 51 days. In addition to basic test controls recorded prior to swimming, further basic test (BT) recordings were produced for an hour after each session (with short 1–2 min breaks). This led to the experiments based on sports load having 183 basic tests. However, as the adaptive changes under sports load were recorded on a volunteer without prior athletic training, only data from 20 basic tests ($n = 20$) recorded in the first two weeks of training were used for analysis and calculation of oxygen consumption. This volunteer's studies were also conducted in the skin without AVAs ($n = 41$).

The female participant (volunteer no 2) was studied over the course of one month, totalling 39 studies only in the skin with AVAs: 19 basic tests for 3 min plus 20 occlusion tests with an occlusion for 1 min followed by a 3 min post occlusion period. Occlusion tests were performed according to standard procedures: the volunteer was in a sitting position (forearm, at heart level), the cuff of the tonometer was located on the upper arm near the area of the shoulder and the cuff was pumped to a pressure of 220–230 mmHg. The occlusion was used to induce adaptive changes in the volunteer. These occlusion tests were carried out on the same day as the basic tests, after a period of 20–30 min rest.

For the remaining volunteers (no 3–8), only basic tests were performed on both points of interest (skin with and without AVAs) and they were not subjected to additional stress. Studies of these volunteers were carried out five times a week (when possible) at around the same time of day, and always followed the methodology described above. Measurements were carried out under conditions of physiological dormancy and non-physiological rest (physical or emotional and psychological stress). It is important to note that all volunteers prior to testing were questioned about their psychoemotional state and were recorded as either normal or under emotional stress.

Wavelet analysis was performed on five rhythmic components (oscillations) of I_m - and S_tO_2 -records, namely endothelial (0.0095–0.02 Hz); neurogenic (0.02–0.06 Hz); myogenic (0.06–0.16 Hz); breathing (0.16–0.4 Hz) and pulse (0.4–1.6 Hz) (Stefanovska *et al* 1999, Kvandal *et al* 2006, Krupatkin 2008, 2009). For the purposes of this investigation, however, the endothelial component was not required. The typical forms of perfusion and tissue oxygen saturation are shown in figure 2(a) and the results of the wavelet analysis for them during the basic test are presented in figure 2(b).

Of particular interest is the analysis and comparison of oxygen consumption in tissue under normal conditions and during adaptive changes, accompanied by sympathetic vasomotor reflex (synchronization and resonance of the myogenic oscillation in perfusion and tissue oxygen saturation). This is especially interesting as a relationship between the activation of vasomotion and oxygen consumption has been previously identified (Kislukhin 2004). According to the methodology thoroughly explained in the paper (Krupatkin 2012) and using data from the spectral wavelet analysis of I_m - and S_tO_2 -graphs, we have calculated the extraction and consumption of oxygen in tissue for all eight volunteers. It should be noted that what we understand of general oxygen saturation oscillations and particularly of myogenic rhythms is as follows. Myogenic oscillations of oxygen saturation we consider primarily as oxygen saturation changes in light of the changes in tissue oxygen consumption. These changes correspond to the oscillations of blood flow in the myogenic range. As stated above the tissue oxygen saturation is determined by a spectrophotometric method. In fact, this value undergoes changes primarily during the modulation of blood flow as a result of the oscillations of perfusion due to the myogenic regulation of microvascular tone. Thus, the oxygen saturation value oscillations primarily depend on the blood flow oscillations resulting from changes in the microvascular tone.

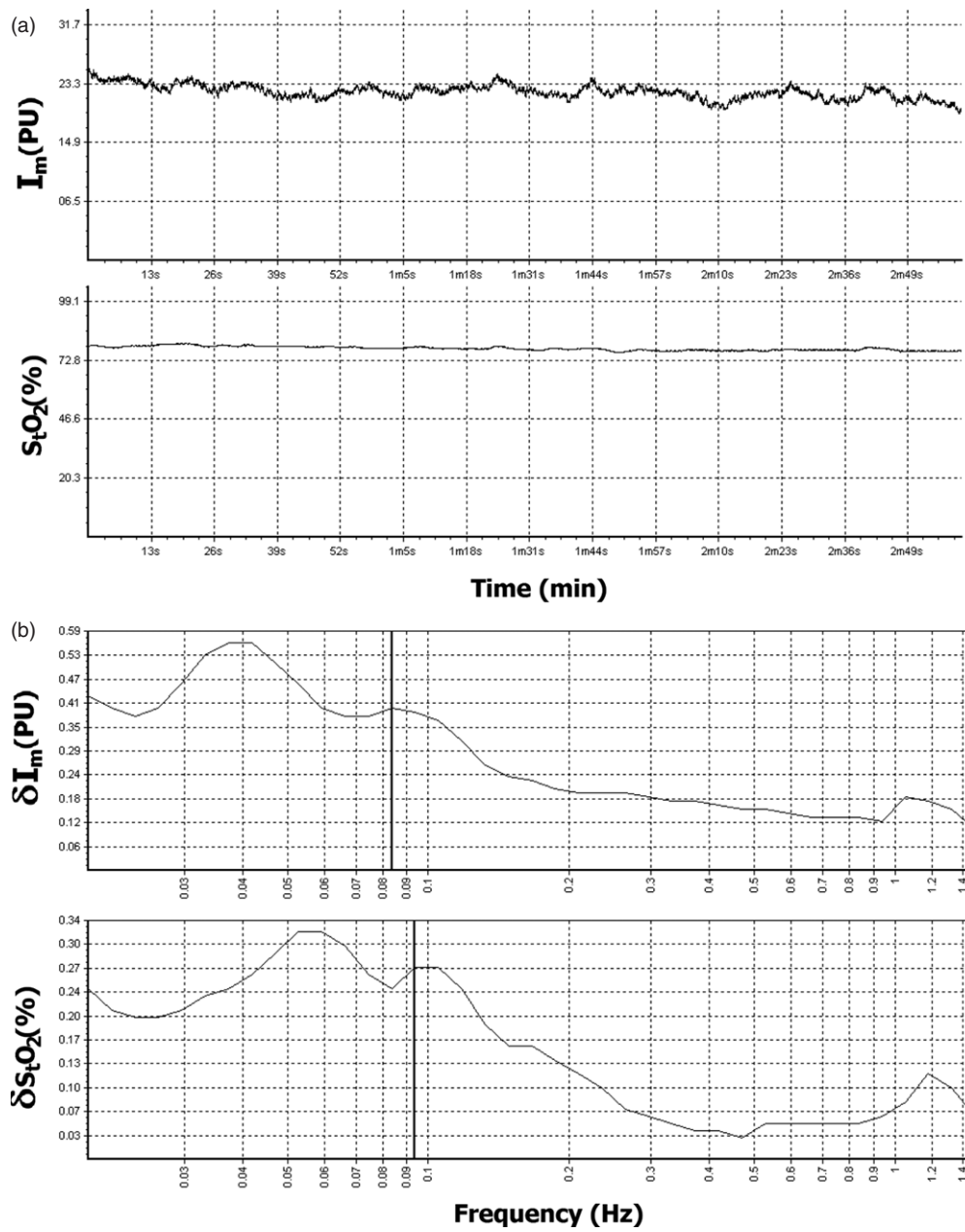


Figure 2. (a) The typical form of perfusion and tissue oxygen saturation graphs, measured using LDF and TRO, respectively and (b) wavelet analysis results following such basic tests, where δI_m —amplitude of perfusion oscillations, δS_tO_2 —amplitude of oxygen saturation oscillations. Furthermore, in (b), a line is used to represent the amplitude oscillation of microvascular blood flow $(\delta I_m)_m = 0.40$ PU at a frequency of $f_m = 0.084$ Hz and tissue oxygen saturation $(\delta S_tO_2)_m = 0.27\%$ at a frequency of $f_m = 0.094$ Hz for myogenic rhythms.

Oxygen extraction (OE), assessed in arbitrary units (AU), was calculated as follows:

$$OE = \frac{S_aO_2 - S_vO_2}{S_aO_2}, \tag{6}$$

where S_vO_2 is the venous blood oxygen saturation, calculated using spectral wavelet analysis of tissue oxygen saturation changes. We also analyzed the amplitude of tissue oxygen saturation changes $(\delta S_tO_2)_c$, topographically linked to the influent blood of the microvasculature (predominantly cardiac rhythms), and the amplitude of tissue oxygen saturation changes $(\delta S_tO_2)_r$, topographically linked to the effluent blood of the microvasculature (predominantly respiratory rhythms). If the $(\delta S_tO_2)_c/(\delta S_tO_2)_r$ ratio ≤ 1 , then S_vO_2 is taken to be equal to S_tO_2 . This variant predominates in most cases of recordings from the skin without AVAs. If the $(\delta S_tO_2)_c/(\delta S_tO_2)_r$ ratio > 1 , then:

$$S_vO_2 = \frac{S_tO_2}{(\delta S_tO_2)_c/(\delta S_tO_2)_r}. \tag{7}$$

This variant predominates in most cases of recordings from the skin with AVAs. In the cases of resonance in oxygen saturation changes in the active frequency bands (for example, in the myogenic range during adaptive changes), the value $(\delta S_tO_2)_c$ and $(\delta S_tO_2)_r$ may not be expressed in the spectrum, and the S_vO_2 calculation has some specific features. In the cases of resonance in oxygen saturation changes in the total myogenic and respiratory bands, $S_vO_2 = S_tO_2$. In the skin zones with AVAs, an additional factor, the bypass index (BI) for S_tO_2 , is necessary:

$$S_vO_2 = \frac{S_tO_2}{BI(S_tO_2)}, \tag{8}$$

where:

$$BI(S_tO_2) = 1 + \frac{(\delta S_tO_2)_n}{(\delta S_tO_2)_m}, \tag{9}$$

where $(\delta S_tO_2)_n$ and $(\delta S_tO_2)_m$ are amplitudes of oxygen saturation changes in neurogenic and myogenic rhythms respectively.

Oxygen consumption (OC), assessed in arbitrary units (AU), was calculated as follows:

$$OC = I_{mn} \cdot (S_aO_2 - S_vO_2), \tag{10}$$

where I_{mn} is the nutritive blood flow value was calculated according to the equation:

$$I_{mn} = \frac{I_m}{BI(I_m)}, \tag{11}$$

where $BI(I_m)$ is the bypass index is calculated for skin with AVAs similarly to formula (9), but only using perfusion data. For skin zones without AVAs:

$$BI(I_m) = \frac{(\delta I_m)_{max}}{(\delta I_m)_m}, \tag{12}$$

where $(\delta I_m)_{max}$ is the maximum amplitude of the dominant oscillations in the active range of frequencies up to 0.15 Hz and $(\delta I_m)_m$ is amplitude of oscillations of myogenic rhythms.

Features involved in the calculation of oxygen consumption in cases with adaptive changes (for synchronization and resonance of myogenic oscillations in perfusion and oxygen saturation changes) were processed separately. It should be noted that the OC equation includes the perfusion rate value, due to which the OC value (calculated according to Fick's principle) reflects the oxygen consumption rate.

Furthermore, the normalized amplitude of myogenic rhythms was calculated using the standard deviation of perfusion and of tissue oxygen saturation, respectively:

$$(\delta I_m)'_m = \frac{(\delta I_m)_m}{\sigma_{per}}; \quad (\delta S_tO_2)'_m = \frac{(\delta S_tO_2)_m}{\sigma_{sat}}, \tag{13}$$

Table 2. The results of measurements in the skin with AVAs and calculation of oxygen extraction and consumption for volunteer no 1.

No	Parameters	State		
		Norm ($n = 59$)	With adaptive changes: stress ($n = 21$)	With adaptive changes: sport ($n = 20$)
1	$I_m(\text{total})$, PU	20.8 ± 2.7	20.3 ± 3.1	20.3 ± 2.4
2	$I_{mn}(\text{nutritive})$, PU	8.4 ± 1.6	10.6 ± 1.9^a	11.5 ± 1.3^a
3	S_aO_2 , %	98.1 ± 0.5	97.9 ± 0.5	97.7 ± 0.5
4	S_tO_2 , %	76.1 ± 2.9	75.2 ± 2.8	76.3 ± 4.2
5	S_vO_2 , %	39.8 ± 10.3	41.2 ± 5.5	41.7 ± 5.5
6	V_b , %	9.9 ± 0.9	10.0 ± 0.9	10.4 ± 0.8
7	$(\delta I_m)'_m$, AU	0.44 ± 0.14	0.54 ± 0.15^b	0.61 ± 0.14^b
8	$(\delta S_tO_2)'_m$, AU	0.39 ± 0.15	0.44 ± 0.15	0.54 ± 0.21^b
9	$f_m(\delta I_m)$, Hz	0.071 ± 0.012	0.077 ± 0.019^b	0.092 ± 0.015^b
10	$f_m(\delta S_tO_2)$, Hz	0.081 ± 0.026	0.092 ± 0.035	0.092 ± 0.014^b
11	$BI(I_m)$, AU	2.5 ± 0.4	1.9 ± 0.2^b	1.8 ± 0.2^b
12	$BI(S_tO_2)$, AU	2.4 ± 0.7	1.8 ± 0.2^b	1.9 ± 0.2^b
13	OE, AU	0.59 ± 0.11	0.58 ± 0.06	0.57 ± 0.06
14	OC, AU	488.6 ± 131	597 ± 109^b	641 ± 91^b

^a Significant difference ($p < 0.05$) observed from normal state, calculated by a t -test.

^b Significant difference ($p < 0.05$) observed from normal state, calculated by the Mann–Whitney test.

where σ_{per} and σ_{sat} are the standard deviation of perfusion and tissue oxygen saturation during a basic test, respectively.

Data presented in the text are means \pm SD. Statistical analysis was performed using OriginPro 8 SRO version v.8.0724 with data sets tested for normality by the Kolmogorov–Smirnov and Shapiro–Wilk tests. For normally distributed data, group comparisons were made by carrying out a parametric unpaired t -test. For the non-normally distributed data, the Mann–Whitney test of nonparametric statistics was used to compare the two groups (normal and with conditions of adaptive changes).

3. Results and discussion

Analysis of the data has demonstrated the emergence of synchronization and resonance of vasomotion in microvascular blood flow and oxygen saturation only in the range of myogenic oscillation during adaptive changes—for example, stressful situations or reaction to sports load. The typical form of perfusion and tissue oxygen saturation, along with the results of wavelet analysis of these parameters during adaptive changes, are presented in figure 3.

The parameters for calculating oxygen extraction and consumption for all volunteers were obtained using the approaches detailed in the methods section above. The results of measurements in the skin with AVAs and calculations of the parameters of tissue respiration (oxygen extraction and consumption) for volunteer no 1 with the single largest sample of recorded data are shown in table 2. The results of measurements and calculations for both areas studied (skin with and without AVAs) for all the eight volunteers are shown in table 3.

The data received for volunteer no 1 (table 2) presented 41 cases (20 cases of which were after exercise) of synchronization and resonance of vasomotion in microvascular blood flow and oxygen saturation out of a total of 100 recorded measurements of skin containing AVAs. For the total population (table 3), 60 out of 247 measurements of AVA containing skin and 26 out of 154 measurement in AVA free skin were observed to have synchronization.

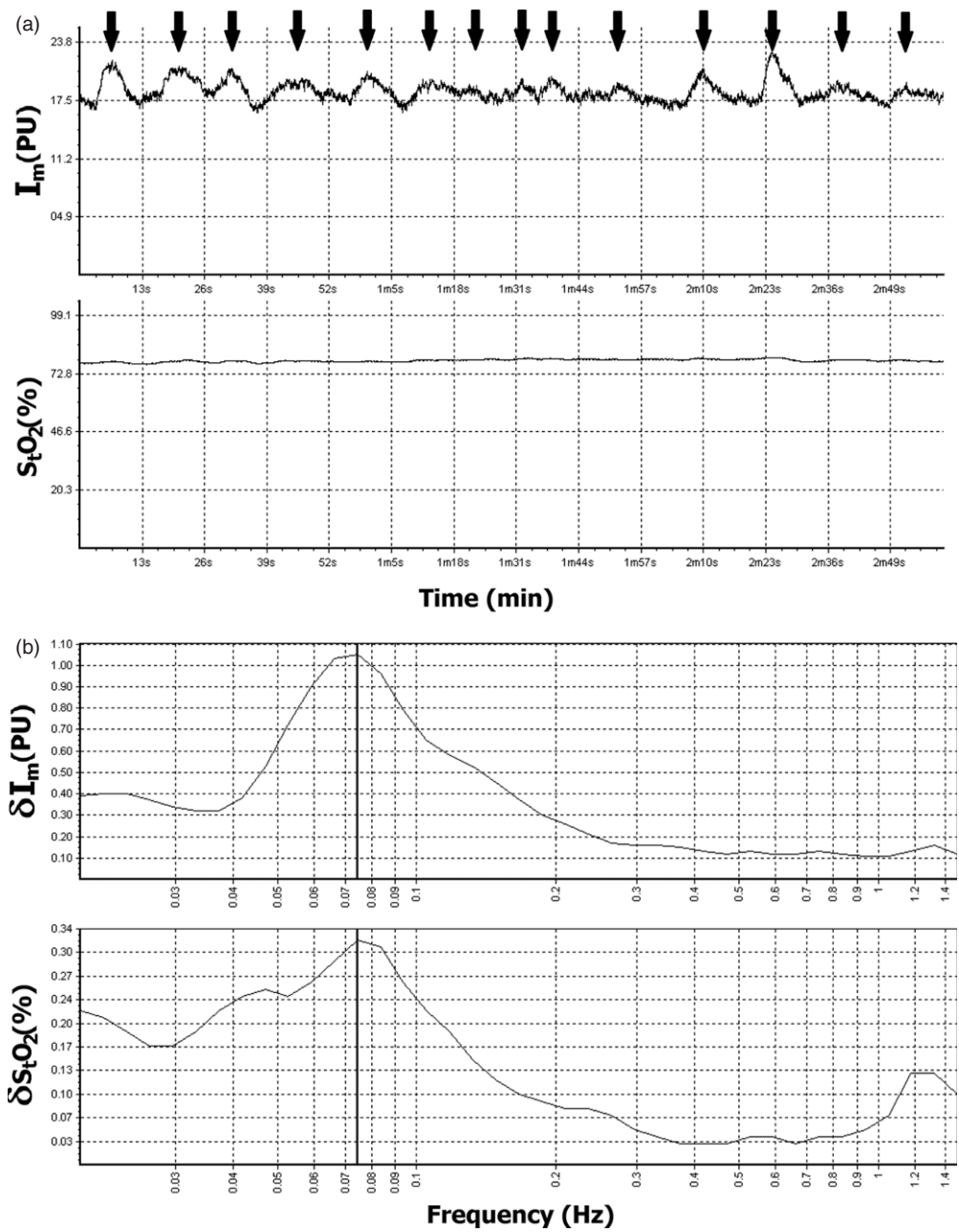


Figure 3. (a) Perfusion and oxygen saturation graphs in cases of myogenic oscillation, represented on the I_m -graph by a \downarrow and (b) typical example of resonance and synchronized rhythms ($f_m = 0.074$ Hz) of microvascular blood flow $(\delta I_m)_m = 1.05$ PU and oxygen saturation $(\delta S_{tO_2})_m = 0.32\%$ within the range of only myogenic oscillation (vasomotion) during adaptive changes.

Table 3. The results of measurements and calculations for all eight volunteers.

No	Parameters	Skin with AVAs		Skin without AVAs	
		Norm (<i>n</i> = 187)	With adaptive changes (<i>n</i> = 60)	Norm (<i>n</i> = 128)	With adaptive changes (<i>n</i> = 26)
1	I_m (total), PU	21.0 ± 3.1	21.4 ± 3.4	2.5 ± 0.8	2.8 ± 0.9
2	I_{mn} (nutritive), PU	8.6 ± 0.5	11.1 ± 2.2 ^a	1.7 ± 0.8	2.8 ± 0.8 ^b
3	S_aO_2 , %	98.1 ± 0.4	97.9 ± 0.4	97.9 ± 0.4	97.8 ± 0.6
4	S_iO_2 , %	78.3 ± 4.7	77.7 ± 5.7	66.2 ± 9.3	61.9 ± 7.3
5	S_vO_2 , %	41.6 ± 13.7	41.9 ± 6.1	58.2 ± 12.7	61.3 ± 7.3
6	V_b , %	10.2 ± 1.8	9.9 ± 1.5	6.3 ± 1.7	6.0 ± 1.4
7	$(\delta I_m)'_m$, AU	0.44 ± 0.13	0.52 ± 0.13 ^b	0.46 ± 0.13	0.67 ± 0.11 ^b
8	$(\delta S_iO_2)'_m$, AU	0.33 ± 0.15	0.41 ± 0.17 ^b	0.25 ± 0.13	0.77 ± 0.19 ^b
9	$f_m(\delta I_m)$, Hz	0.086 ± 0.023	0.084 ± 0.025	0.089 ± 0.018	0.086 ± 0.021
10	$f_m(\delta S_iO_2)$, Hz	0.091 ± 0.029	0.093 ± 0.035	0.090 ± 0.019	0.084 ± 0.021 ^b
11	BI(I_m), AU	2.5 ± 0.5	1.9 ± 0.2 ^b	1.6 ± 0.6	1.0 ± 0.06 ^b
12	BI(S_iO_2), AU	2.7 ± 0.7	1.9 ± 0.2 ^b	2.4 ± 1.6	1.0 ± 0.2 ^b
13	OE, AU	0.58 ± 0.14	0.57 ± 0.06	0.41 ± 0.13	0.37 ± 0.07
14	OC, AU	495 ± 170	617 ± 123 ^b	69 ± 40	102 ± 38 ^b

^a Significant difference ($p < 0.05$) observed from normal state, calculated by a *t*-test.

^b Significant difference ($p < 0.05$) observed from normal state, calculated by the Mann–Whitney test.

The human skin contains functionally distinct zones, differing in morphological properties and the regulation of microvascular blood flow. These can be classified as with and without the presence of AVAs. The zones with AVAs are functionally tied to the implementation of thermoregulatory homeostasis and are almost exclusively regulated by the sympathetic adrenergic nervous system. Additionally, the values of perfusion and intravascular pressure of the skin microvessels is generally higher in regions containing AVAs. The zones of skin without AVAs are characterized by lower blood flow in microvessels and a higher contribution of the venous component. As the data of tables 2 and 3 show, during adaptive changes, a significant increase in the nutritive perfusion (I_{mn}) is observed in the zones with AVAs: for example, for volunteer no 1— 8.4 ± 1.6 PU versus 10.6 ± 1.9 PU, $p < 0.05$ (for stress) and 8.4 ± 1.6 PU versus 11.5 ± 1.3 PU, $p < 0.05$ (for sport); and for all volunteers— 8.6 ± 0.5 PU versus 11.1 ± 2.2 PU $p < 0.05$ (for stress). Oxygen extraction did not change in the zones with and without AVAs. Increasing oxygen consumption was therefore due to an increase in perfusion rather than an increase in OE, thus adaptive changes naturally lead to the intensification of oxygen consumption in zones with AVAs: for example, for volunteer no 1— 488.6 ± 131 AU versus 597 ± 109 , $p < 0.05$ (for stress) and 488.6 ± 131 AU versus 641 ± 91 AU, $p < 0.05$ (for sport); for all volunteers— 495 ± 170 AU versus 617 ± 123 AU, $p < 0.05$ (for stress). More cases of synchronization of myogenic rhythms of microvascular blood flow and oxygen saturation were observed in zones with AVAs, this is most likely due to the larger numbers of autonomic nerves, which are very responsive to adaptive changes. Additionally, adaptive changes caused by sport were manifested more clearly during the early stages of physical training (first 2–3 weeks). This may be due to an adaptation of the microcirculatory system to the physical loads upon the organism.

The results from our studies on adaptive changes (stress- or exercise-induced) support our hypothesis that during resonance and synchronization of blood flow oscillations and oxygen saturation changes via myogenic oscillation there is increased tissue oxygen consumption compared with normal conditions. Thus, extraction of oxygen remains unchanged. In all cases the bypass index reduced under conditions of stress and exercise, thereby confirming reduced circulatory AVAs as one healthy physiological response to stress.

Table 4. Individual cases of adaptive changes per volunteer.

No volunteer	With AVAs		Without AVAs	
	Adaptive changes	Total	Adaptive changes	Total
1	41	99	7	41
2	5	39	-	-
3	4	23	1	5
4	4	18	4	14
5	11	27	0	25
6	9	34	9	31
7	2	22	3	21
8	3	25	2	17

Therefore, we suggest that the bypass index may be used as a marker of adaptive changes (indicating stress conditions), calculated based on perfusion and tissue oxygen saturation.

The increase in amplitude of myogenic rhythm reflects a modulation of the hydrostatic pressure in the capillaries, resulting in an increase in diffusion of oxygen into the tissues, hence the changes in tissue oxygen saturation. Time shifts and frequency characteristics are obviously specific to particular individuals. For example, the number of recorded cases of adaptive changes for each volunteer is presented in table 4.

Analysis of recorded time fragments under normal conditions, during stress and following exercise presented distinct differences in the frequency of myogenic oscillations in perfusion and tissue oxygen saturation changes. As the data on tables 2 and 3 show, the frequency of oxygen saturation changes corresponding to the oscillations of blood flow in the myogenic range and the vasomotion in perfusion both increase under adaptive changes (heading towards the so-called central frequency of myogenic oscillations—0.1 Hz). This is particularly expressed in the case of the reaction to sports load for volunteer no 1 with perfusion 0.071 ± 0.012 Hz versus 0.092 ± 0.015 Hz, $p < 0.05$ and tissue oxygen saturation 0.081 ± 0.026 Hz versus 0.092 ± 0.014 Hz, $p < 0.05$. This is likely the result of higher levels of adaptive change causing more intense and clear synchronization of vasomotion. Occasionally, complete synchronization will be achieved when the frequency of both myogenic oscillations coincide. For example, this case is presented in figure 4.

The analysis of data presented in tables 2 and 3 also shows that normalized perfusion vasomotion amplitudes (for example in the regions with AVA for all volunteers— 0.44 ± 0.13 AU versus 0.52 ± 0.13 , $p < 0.05$) and tissue oxygen saturation (0.33 ± 0.15 AU versus 0.41 ± 0.17 , $p < 0.05$) increase under adaptive changes. This is the result of these amplitudes shifting towards synchronization at the microcirculatory level to maintain homeostasis in the oxygen delivery and consumption system. These cases demonstrate increased blood flow and oxygen into the nutritive flux, which is reflected in the spectrum as a rise in myogenic oscillations amplitude. The oxygen delivered to the nutritive flux can move into tissues and be consumed in the process of metabolism. This results in an increasing OC and/or OE. If the tissue exchange is not active, the oxygen may be shunted. This is particularly visible in areas without AVAs, where the shunting happens via major vessels. In this circumstance, however, OC and/or OE do not rise or fall despite an increase in myogenic amplitudes to a resonance within the spectrum (for example, for the perfusion of all volunteers 0.46 ± 0.13 AU versus 0.67 ± 0.11 AU, $p < 0.05$ and for the tissue oxygen saturation 0.25 ± 0.13 AU versus 0.77 ± 0.19 AU, $p < 0.05$).

Data analysis has demonstrated an increase in resonance and synchronization of microvascular blood flow and oxygen saturation rhythms as an adaptive change in myogenic

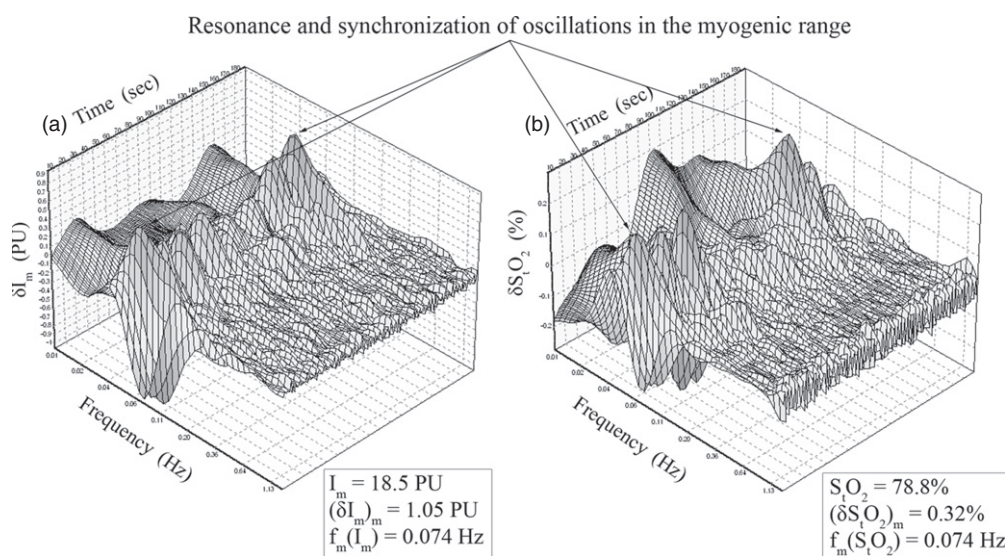


Figure 4. Typical example of the 3D wavelet analysis of resonating and synchronized myogenic rhythms of microvascular blood flow (a) and oxygen saturation changes (b) during adaptive changes.

oscillation (vasomotion) resulting from exercise and potentially from psychoemotional stress. An explanation for this observed response may be that the synchronization of myogenic rhythms facilitates maximum oxygen delivery to tissue following or during periods of physical or emotional stress. The data obtained show differences in myogenic oscillations in both the ordinary state of the body (normality) and during episodes of sympathoadrenal activation (e.g. emotional stress). Normally, all systems of the body (including blood circulation, respiration, metabolism, etc) work in different phases and frequencies, exhibiting non-linearity and independence. Synchronization of myogenic rhythms during adaptive changes may promote increased oxygen consumption resulting from increased microvascular blood flow velocity. The data above indicate that adaptive changes lead to the intensification of oxygen consumption in zones with AVAs due to an increased perfusion. Furthermore, as these zones have rich autonomic innervation, they are very sensitive to adaptive change leading to them having a higher incidence of myogenic rhythm synchronization of microvascular blood flow and oxygen saturation. During adaptive changes (under particular emotional stress, etc), synchronization increases, reducing the freedom of microvascular blood flow regulation.

Ultimately, our suggested approaches for the use of the laser technology in investigating tissue respiration and skin microhaemocirculation under adaptive changes, through the use of the synchronization of blood flow and oxygen saturation rhythms observed within the data, have shown themselves to be highly informative of the response of the microcirculation system and offers interesting prospects for further investigation as a potential diagnostic methodology relevant to vascular function. The studied parameters of microcirculatory regulation, particularly under stresses and adaptive changes, may present a diagnostic approach when developing control methods for various disease treatments and may provide a window to examine the condition and function of the overall respiratory and cardiovascular systems. It is likely to offer particular utility in monitoring of cardiovascular function, such as response to treatment efficacy in patients with arterial hypertension. Further potential applications in the fields of sports medicine and the assessment of neurological disorders could also be considered.

Acknowledgments

We would like to thank all of our volunteers for their contribution to this research project. This work was supported by the European Community's Seventh Framework Programme (FP7-People-2009-IAPP) under grant agreement no 251531 MEDILASE.

References

- Amzina M V, Micheev A A, Rogatkin D A and Sidorov V V 2006 Combined medical diagnostic system with separated laser-Doppler and reflectance oximeter channels *Proc. SPIE* **6163** 616317
- Bernjak A, Stefanovska A, McClintock P V E, Owen-Lynch P J and Clarkson P B M 2012 Coherence between fluctuations in blood flow and oxygen saturation *Fluctuation Noise Lett.* **11** 1240013
- Bernjak A, Stefanovska A, Urbancic-Rovan V and Azman-Juvan K 2005 Quantitative assessment of oscillatory components in blood circulation: classification of the effect of ageing, diabetes and acute myocardial infarction *Proc. SPIE* **5692** 163–73
- Bracic M and Stefanovska A 1998 Wavelet-based analysis of human blood-flow dynamics *Bull. Math. Biol.* **60** 919–35
- Coca D, Zheng Y, Mayhew J E W and Billings S A 1998 Non-linear analysis of vasomotion oscillations in reflected light measurements *Oxygen Transport to Tissue Xx* ed A G Hudetz and D F Bruley (New York: Plenum)
- Coca D, Zheng Y, Mayhew J E W and Billings S A 2000 Nonlinear system identification and analysis of complex dynamical behavior in reflected light measurements of vasomotion *Int. J. Bifurcation Chaos* **10** 461–76
- Colquhoun D, Tucker-Schwartz J, Durieux M and Thiele R 2012 Non-invasive estimation of jugular venous oxygen saturation: a comparison between near infrared spectroscopy and transcutaneous venous oximetry *J. Clin. Monit. Comput.* **26** 91–8
- Daly S M, Silien C and Leahy M J 2013 Optimization and extraction of functional information from *in vitro* flow models using dual-beam spectral-domain optical coherence tomography cross-correlation analysis *J. Biomed. Opt.* **18** 106003
- Dunaev A V, Sidorov V V, Stewart N A, Sokolovski S G and Rafailov E U 2013 Laser reflectance oximetry and Doppler flowmetry in assessment of complex physiological parameters of cutaneous blood microcirculation *Proc. SPIE* **8572** 857205
- Fine I, Kaminsky A, Kuznik B and Shenkman L 2012 A non-invasive method for the assessment of hemostasis *in vivo* by using dynamic light scattering *Laser Phys.* **22** 469–75
- Graaff R, Morales F, Smit A J, De Jong E D, De Mul F F M and Rakhorst G 2007 Normalization of vasomotion in laser Doppler perfusion monitoring *Proc. IEEE 2007 Annu. Int. Conf. of the IEEE Engineering in Medicine and Biology Soc.* pp 4076–9
- Heusmann H, Koelzer J G and Mitic G 1996 Characterization of female breasts *in vivo* by time-resolved and spectroscopic measurements in the near infrared spectroscopy *J. Biomed. Opt.* **1** 425–34
- Kalchenko V, Kuznetsov Y, Meglinski I and Harmelin A 2012 Label free *in vivo* laser speckle imaging of blood and lymph vessels *J. Biomed. Opt.* **17** 050502
- Kalchenko V, Madar-Balakirski N, Meglinski I and Harmelin A 2011 *In vivo* characterization of tumor and tumor vascular network using multi-modal imaging approach *J. Biophotonics* **4** 645–9
- Khalil O S 2006 Metabolites, noninvasive optical measurements of *Wiley Encyclopedia of Biomedical Engineering* ed M Akay (New York: Wiley)
- Kislukhin V V 2004 Regulation of oxygen consumption by vasomotion *Math. Biosci.* **191** 101–8
- Krupatkin A I 2007 Dynamic oscillatory circuit of regulation of capillary hemodynamics *Hum. Physiol.* **33** 595–602
- Krupatkin A I 2008 Cardiac and respiratory oscillations of the blood flow in microvessels of the human skin *Hum. Physiol.* **34** 323–9
- Krupatkin A I 2009 Blood flow oscillations at a frequency of about 0.1 Hz in skin microvessels do not reflect the sympathetic regulation of their tone *Hum. Physiol.* **35** 183–91
- Krupatkin A I 2011 The problem of information value in microvascular networks *Hum. Physiol.* **37** 312–7
- Krupatkin A I 2012 Noninvasive estimation of human tissue respiration with wavelet-analysis of oxygen saturation and blood flow oscillations in skin microvessels *Hum. Physiol.* **38** 396–401
- Krupatkin A I, Rogatkin D A and Sidorov V V 2007 Clinical-diagnostic parameters for complex investigation of microhaemodynamics and oxygen transport in the system of microcirculation *2007 Int. Conf. on Hemorheology and Microcirculation (Yaroslavl, Russia)* p 106

- Krupatkin A I and Sidorov V V (ed) 2005 *Laser Doppler Flowmetry of Blood Microcirculation* (Moscow: Medicina-Press)
- Kvandal P, Landsverk S A, Bernjak A, Stefanovska A, Kvernmo H D and Kirkeboen K A 2006 Low-frequency oscillations of the laser Doppler perfusion signal in human skin *Microvasc. Res.* **72** 120–7
- Kvernmo H D, Stefanovska A, Kirkeboen K A and Kvernebo K 1999 Oscillations in the human cutaneous blood perfusion signal modified by endothelium-dependent and endothelium-independent vasodilators *Microvasc. Res.* **57** 298–309
- Leahy M J and Nilsson G E 2010 Laser Doppler flowmetry for assessment of tissue microcirculation: 30 years to clinical acceptance *Proc. SPIE* **7563** 75630E
- Newman J M B, Dwyer R M, St-Pierre P, Richards S M, Clark M G and Rattigan S 2009 Decreased microvascular vasomotion and myogenic response in rat skeletal muscle in association with acute insulin resistance *J. Physiol. Lond.* **587** 2579–88
- Obeid A N 1993 In vitro comparison of different signal-processing algorithms used in laser doppler flowmetry *Med. Biol. Eng. Comput.* **31** 43–52
- Quaresima V, Ferrari M and Fantini S 2013 Accuracy of oxygen desaturation of hemoglobin in muscle by near-infrared oximeters *Med. Sci. Sports Exerc.* **45** 1217
- Rogatkin D A, Dunaev A V and Lapaeva L G 2010 Metrological support of methods and devices for noninvasive medical spectrophotometry *Biomed. Eng.* **44** 66–70
- Rogatkin D A and Lapaeva L G 2003 Prospects for development of non-invasive spectrophotometry medical diagnostics *Biomed. Eng.* **37** 217–22
- Rogatkin D A, Sokolovski S G, Fedorova K A, Sidorov V V, Stewart N Z and Rafailov E U 2011 Basic principles of design and functioning of multifunctional laser diagnostic system for non-invasive medical spectrophotometry *Proc. SPIE* **7890** 78901H1
- Rossi M, Carpi A, Galetta F, Franzoni F and Santoro G 2008 Skin vasomotion investigation: a useful tool for clinical evaluation of microvascular endothelial function? *Biomed. Pharmacother.* **62** 541–5
- Rossi M, Matteucci E, Pesce M, Consani C, Galetta F, Giampietro O and Santoro G 2013 Study of skin vasomotion in type 1 diabetic patients and of its possible relationship with clinical and laboratory variables *Clin. Hemorheol. Microcirc.* **53** 357–67
- Salerud E G, Tenland T, Nilsson G E and Oberg P A 1983 Rhythmical variations in human skin blood flow *Int. J. Microcirc.: Clin. Exp.* **2** 91–102
- Schmidt-Lucke C, Borgstrom P and Schmidt-Lucke J A 2002 Low frequency flowmotion/(vasomotion) during patho-physiological conditions *Life Sci.* **71** 2713–28
- Schmiedel O, Schroeter M L and Harvey J N 2007 Microalbuminuria in type 2 diabetes indicates impaired microvascular vasomotion and perfusion *Am. J. Physiol.: Heart Circ. Physiol.* **293** H3424–31
- Stefanovska A 2009 Dynamics of blood oxygenation gives better insight into tissue hypoxia than averaged values *Am. J. Physiol.: Heart Circ. Physiol.* **296** H1224–6
- Stefanovska A, Bracic M and Kvernmo H D 1999 Wavelet analysis of oscillations in the peripheral blood circulation measured by laser Doppler technique *IEEE Trans. Biomed. Eng.* **46** 1230–9
- Stewart N A, Dunaev A V, Sokolovski S G, Sidorov V V and Rafailov E U 2012 Multi-parameter analysis in blood circulation and perfusion based diagnostics 2012 *Int. Conf. Laser Optics (St. Petersburg, Russia)* pp 25–9
- Tankanag A and Chemeris N 2008 Application of the adaptive wavelet transform for analysis of blood flow oscillations in the human skin *Phys. Med. Biol.* **53** 5967–76
- Tankanag A V and Chemeris N K 2009 A method of adaptive wavelet filtering of the peripheral blood flow oscillations under stationary and non-stationary conditions *Phys. Med. Biol.* **54** 5935–48
- Thorn C E, Kyte H, Slaff D W and Shore A C 2011 An association between vasomotion and oxygen extraction *Am. J. Physiol.: Heart Circ. Physiol.* **301** H442–9
- Thorn C E, Matcher S J, Meglinski I V and Shore A C 2009 Is mean blood saturation a useful marker of tissue oxygenation? *Am. J. Physiol.: Heart Circ. Physiol.* **296** H1289–95
- Tyrrell J, Thorn C, Shore A, Campbell S and Curnow A 2011 Oxygen saturation and perfusion changes during dermatological methylaminolaevulinate photodynamic therapy *Br. J. Dermatol.* **165** 1323–31
- Zakharov P, Dewarrat F, Caduff A and Talary M S 2011 The effect of blood content on the optical and dielectric skin properties *Physiol. Meas.* **32** 131
- Zakharov P, Talary M S and Caduff A 2009 A wearable diffuse reflectance sensor for continuous monitoring of cutaneous blood content *Phys. Med. Biol.* **54** 5301